JOURNAL OF MATERIALS SCIENCE 25 (1990) 3739–3745

# Sol–gel processing and structural study of a vitreous polysiloxane doped with titanium

I. GAUTIER-LUNEAU, A. MOSSET, J. GALY
*CEMES-LOE, 29 rue J. Marvig, 31077 Toulouse Cedex, France*

H. SCHMIDT
*Fraunhofer Institut für Silicatforschung Neunerplatz 2, 8700 Würzburg, FRG*

Monolithic crack-free condensates have been synthesized by hydrolysis and polycondensation of tetraethoxytitanium(IV) and γ-glycidoxypropyltrimethoxysilane. The local order in these materials has been studied by large angle X-ray scattering (LAXS) as well as the influence of $Ti^{4+}$–$Ti^{3+}$ transition induced by UV irradiation. The polysiloxane is characterized by a quasi-regular arrangement of the side-chains similar to the proposed models for liquid-crystalline polysiloxane. Titanium atoms, in an octahedral environment, are coordinated to the diol functions. If the metal percentage is higher than 20%, the titanium atoms are distributed on several sites.

## 1. Introduction

The sol–gel process is generally used to produce purely inorganic glasses, glass–ceramics or ceramics, such as silica glasses or alumina powders. These materials can be obtained as monolithic solids, thin coatings or powders with a controlled morphology. In order to remove the organic residues, the organic group in the starting products are generally hydrolysable.

The use of unhydrolysable ≡Si–C≡ bonded ligands leads to organically modified silicates and offers the possibility of combining "inorganic" and "organic" networks [1]. Philipp and Schmidt [2] distinguish two basic types of organically modified silicates: an inorganic network containing a $R_nSiO_{(4-n)/2}$ ($n = 0,3$) organic network modifier or an organic network covalently bound to an inorganic one.

Such hybrids, which incorporate polydimethylsiloxane with tetraethoxysilane, have been prepared and studied for mechanical properties [3, 4]. The recent development, by Schmidt and coworkers [5, 6] of new materials for hard contact lenses has fully demonstrated the potentialities of this new route.

The mixture of a commercial epoxysilane, γ-glycidoxypropyltrimethoxysilane, and 5 to 20 mol % tetraethoxytitanium(IV) yields monolithic condensates with remarkable wettability and oxygen-permeability characteristics. The incorporation of crosslinking elements such as polymethacrylates greatly improves the mechanical properties whereas the above-mentioned properties remain unchanged.

The study of the binary system, epoxysilane–titanium alkoxyde, is reported hereafter. In a first part, a systematic survey of the preparation conditions leads to an optimized synthesis. The second part of the paper is a tentative modelling of the local order in the amorphous solid from LAXS (large angle X-ray scattering), EXAFS, EPR and FT–NIR results.

## 2. Experimental

### 2.1. Materials preparation

Tetraethoxytitanium(IV) and γ-glycidoxypropyltrimethoxysilane (abbreviated glymo in the text) $(CH_3O)_3Si(CH_2)_3OCH_2CH-CH_2$ (O) are the precursor compounds.

It is well known that under acidic conditions epoxides react with water to give glycols [2]

$$n(CH_3O)_3Si(CH_2)_3OCH_2CH-CH_2 \;(O) \xrightarrow[-CH_3OH]{+H_3O^+} \left[ -O-\underset{\displaystyle O}{\overset{\displaystyle O}{|}}Si-(CH_2)_3OCH_2\underset{\displaystyle OH}{\overset{\displaystyle OH}{|}}CH-CH_2 \right]_n$$

Epoxide polymerization is catalysed by $Ti(OR)_4$. Due to differences in the hydrolysis kinetics of $Ti(OR)_4$ and $R'Si(OR)_3$, however, the condensation may generate Si–O–Si and Si–O–Ti bonds but also, through the glycol function, Si–R′–O–Si and Si–R′–O–Ti bonds. So, hydrolysis and condensation have to be carried out very carefully.

Three preparation procedures have been explored and are summarized in Fig. 1.

The first one uses a large quantity of solvent (ethanol). In this dilute solution, the hydrolysis of $Ti(OR)_4$ leads to the precipitation of $TiO_2$ which cannot be completely redissolved by addition of chlorhydric acid. Thus, it is difficult to control the titanium percentage in the solid. Moreover, the so-obtained material is brittle because of trapped solvent.

The second procedure, without solvent, allows to redissolve the precipitated $TiO_2$ and to obtain

0022–2461/90 $03.00 + .12 

TABLE I Heat treatment

| Temperature (°C) | 60 | 75 | 85 | 95 | 105 | 115 | 125 | 130 |
|---|---|---|---|---|---|---|---|---|
| Heating time (h) | 16 | 4 | 4 | 16 | 4 | 4 | 4 | 4 |

monoliths with a titanium percentage up to 30% molar. In the third one, a prehydrolysis of the glymo is realized adding 1/16 of the stoichiometric quantity of HCl. This addition is followed by a vigorous stirring of the solution during 16 hours. In these conditions, $TiO_2$ does not precipitate; this indicates that titanium atoms are already coordinated to the polymer.

The third synthesis procedure results in monoliths up to 35% molar in titanium.

## 2.2. Heat treatment

The solidification of the materials is realized between 85 and 95° C. The complete heat treatment is indicated in Table I. Transparent monolithic condensates (4 to 7 cm in length and 1.5 cm in diameter) are obtained, free of cracks. The colour varies from colourless to light yellow depending on the titanium percentage.

## 2.3. Elemental analysis

The results are given in Table II. The monolithic samples only have been analysed. The theoretical percentages are calculated in the case of complete hydrolysis reactions. The experimental molar percentages in titanium are also given. They show a better control of the titanium content in the material with the second and third procedures.

## 2.4. FT-NIR spectroscopy

This spectroscopy has been used as a quantitative method to evaluate the percentage of free diol functions. Spectra were recorded on a NICOLET 60 SX FT-NIR spectrometer between 3700 and 6000 $cm^{-1}$. The samples were shaped as thin (0.3 mm) slices of the monoliths.

Diol function presents a characteristic peak at 4800 $cm^{-1}$ (Fig 2). The percentage of free functions can be calculated from the area of this peak

$$C = E/(d\varepsilon)$$

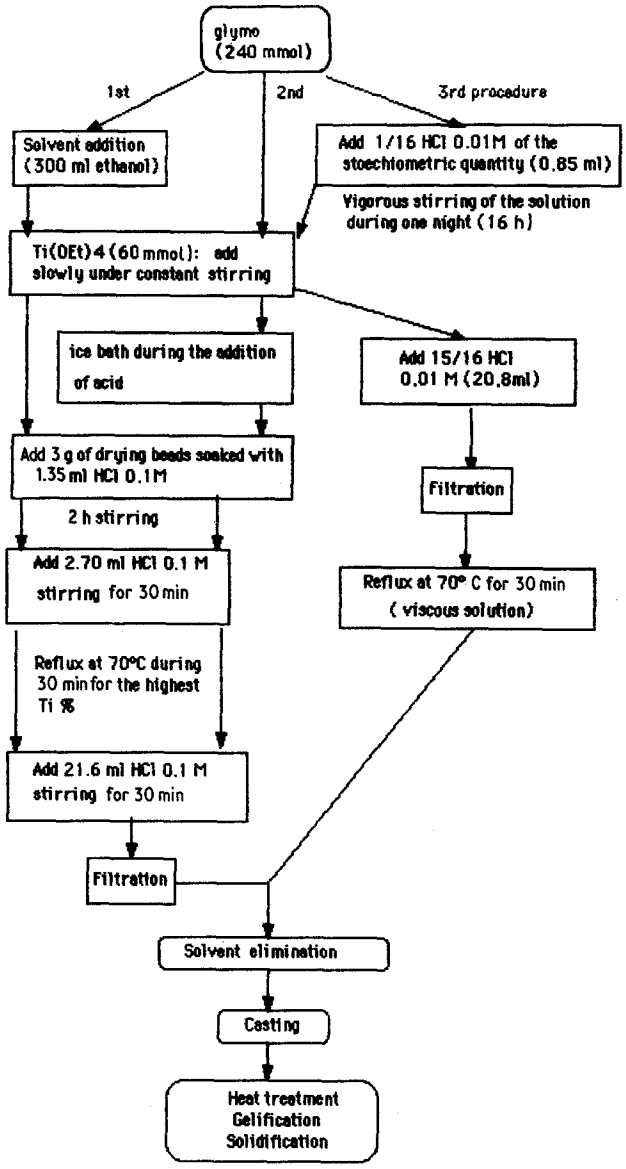


*Figure 1* Scheme of the three synthesis procedures.

where $E$ is the extinction obtained from the peak area, $d$ is the sample thickness and $\varepsilon$ the extinction coefficient, equal to $1.42 \times 10^5$ cm $mol^{-1}$ (this value is calculated using ethoxy-1 propane diol 2-3 as a reference compound). Moreover, if every epoxy group is

TABLE II Elemental analysis

| Molar % Glymo–Ti | Theoretical % (complete hydrolysis) | | | | First method | | | | Second method | | | | Third method | | | |
|---|---|---|---|---|---|---|---|---|---|---|---|---|---|---|---|---|
| | Ti | Si | C | H | Ti | Si | C | H | Ti | Si | C | H | Ti | Si | C | H |
| 100–0 | 0 | 15.41 | 39.54 | 7.19 | | | | | | | | | 0 | 14.7 | 38.31 | 6.98 $\Delta C = 0$ |
| 90–10 | 2.69 | 14.21 | 36.45 | 7.36 | 2.23 %Ti = 8.45 | 13.90 | 39.51 | 6.86 $\Delta C = 6$ | 2.16 %Ti = 8.45 | 13.50 | 38.25 | 6.74 $\Delta C = 5.5$ | 2.46 %Ti = 9.6 | 13.45 | 37.94 | 6.80 $\Delta C = 5.5$ |
| 80–20 | 5.62 | 13.17 | 33.80 | 6.15 | 4.96 %Ti = 17.4 | 13.40 | 38.45 | 6.66 $\Delta C = 5.5$ | 5.27 %Ti = 18.8 | 13.15 | 32.82 | 6.51 $\Delta C = 0$ | 5.10 %Ti = 18.1 | 13.20 | 36.48 | 6.53 $\Delta C = 3.7$ |
| 75–25 | 7.17 | 12.62 | 32.38 | 5.89 | | | | | 6.78 %Ti = 24 | 12.40 | 35.5 | 6.14 $\Delta C = 5$ | 6.35 %Ti = 23 | 12.15 | 35.55 | 6.32 $\Delta C = 6$ |
| 70–30 | 8.80 | 12.04 | 30.90 | 5.62 | | | | | 8.25 %Ti = 27.74 | 12.20 | 34.15 | 6.18 $\Delta C = 4.3$ | 8.32 %Ti = 27.9 | 12.25 | 34.71 | 6.14 $\Delta C = 4.3$ |
| 65–35 | 10.51 | 11.44 | 29.35 | 5.34 | | | | | | | | | 10.16 %Ti = 33 | 11.75 | 33.12 | 5.92 $\Delta C = 3.8$ |

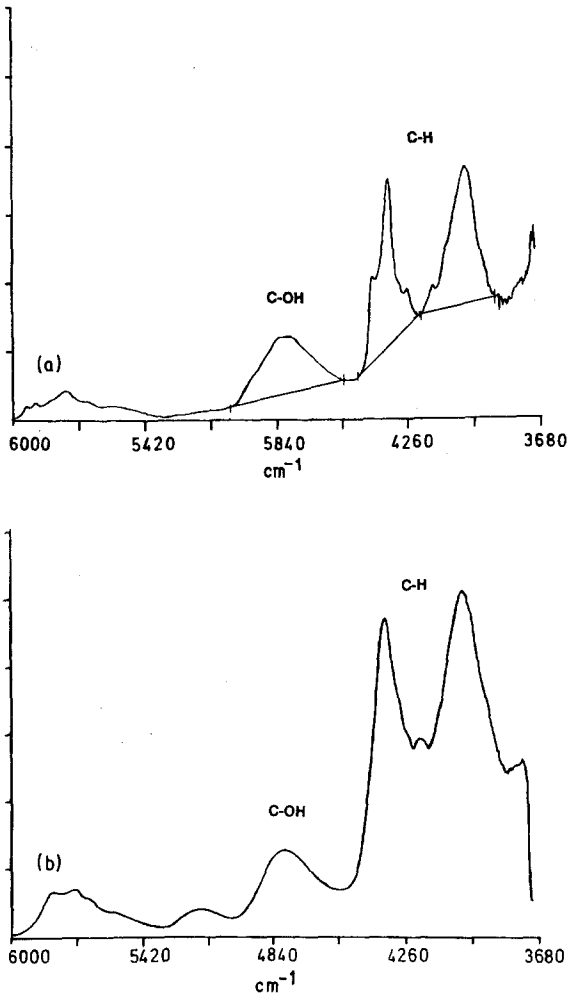


*Figure 2* FT-NIR spectra of (a) the reference compound ($E = 30.27, d = 0.5$ cm, $C = 0.425$ mole$^{-1}$) and (b) a polysiloxane with 10% molar titanium ($E = 12.61$, $d = 0.0275$ cm, $\varepsilon = 1.42 \times 10^5$ cm mol$^{-1}$).

hydrolysed, this concentration should be: $C' = (\rho/M) \cdot n \cdot 10^3$ where $\rho$ is the specific weight. $M$, the molecular weight and $n$, the ratio of epoxyde group in one mole of the compound ($n = 0.9$ in the example shown in Fig. 2b). Thus, the percentage of free diol functions is $100(C/C')$. The so-obtained percentages are equal to 25 to 30% for the first synthesis procedure and 30 to 45% for the second and third ones.

## 2.5. Large angle X-ray scattering (LAXS) studies

Data were collected using the LASIP $\omega$–$\theta$ diffractometer equipped with a position-sensitive detector for the MoK$\alpha$ wavelength [7, 8]. The measurements were carried out at room temperature in the transmission mode. Some 2200 equidistant points were measured within 24 h in the range $1.5° \leqslant \theta \leqslant 66°$. Measuring was performed in an integrative way to minimize the parallax and non-linearity problems of the straight linear position-sensitive detector. All $2\theta$ points were successively run through all the detector channels. At each angular displacement of the detector, an equivalent offset of the channels in the memory is emulated to compensate this movement. This leads to the effect that, at a given $2\theta$ angle, the scattered intensity is always integrated in the same channel. These data were corrected for background, absorption and polarization and normalized following the Krogh-Moe method [9]. Atomic scattering factors were taken from [10], Compton scattering factors from [11]. Treatment of the experimental data led to the radial distribution function (RDF): $F(r) = D(r) - 4\pi\rho_0 r^2$. The experimental RDF was obtained using the relation

$$D(r) = 4\pi\rho_0 r^2 - \frac{2r}{\pi} \int si(s)M(s) \sin(rs)\,ds$$

where $\rho_0$ is the average electron density, $s = 4\pi \sin\theta/\lambda$ ($2\theta$ is the scattering angle), $i(s)$ is the reduced intensity and $M(s)$ a modification function used to down-weight inaccurately known high-angle data and to reduce ripples resulting from termination effects due to the integration. Theoretical intensities were calculated according to Debye's formula [12]

$$i(s)_{th} = \sum\sum f_i(s)f_j(s)(\sin(r_{ij}s)/r_{ij}s) \exp(-b_{ij}s^2)$$

where $i \neq j$, $f(s)$ is the atomic scattering factor corrected for anomalous scattering, $r_{ij}$ is the distance between two atoms and $b_{ij}$ a temperature-related factor influencing the $i$–$j$ interaction. The curve $F(r)_{th}$ is obtained as the Fourier transform

$$F(r) = \frac{2r}{\pi} \int si(s)_{th}M(s) \sin(rs)\,ds$$

## 2.6. EPR measurements

EPR spectroscopy has been used to test the presence of Ti(III) and to study the behaviour of the materials under UV irradiation.

Spectra were recorded in Q band, on solid samples, at room temperature, using a BRUKER 200 TT spectrometer equipped with a BRUKER NMR gaussmeter.

## 2.7. EXAFS measurements

The experiments were realized on the EXAFS I station at LURE-CNRS** (Orsay), using a Si(400) channel-cut monochromator.

Spectra were recorded, for the Ti K edge, on slices (thickness: 1 mm) of the monoliths. $TiO_2$ anatase were used as a model compound to calculate experimental tables.

The radial distribution curves show only one intense peak corresponding to the titanium–oxygen bonds. The best results of the refinement process are given in Table III where $N$ is the number of Ti–O bonds, $R$ the interatomic distance and $\rho$ a reliability coefficient. It can be seen that there is no significant variation of the Ti–O bond length with the titanium percentage.

# 3. Results and discussion

## 3.1. Titanium environment

The modification of the local order has been studied

TABLE III Results of EXAFS experiments

| Ti(%) | $N$ | $R$(nm) | $\rho$(%) |
|---|---|---|---|
| 10 | 6 | 0.186(3) | 0.022 |
| 20 | 6 | 0.185(4) | 0.053 |
| 25 | 6 | 0.188(4) | 0.020 |
| 30 | 6 | 0.188(4) | 0.009 |

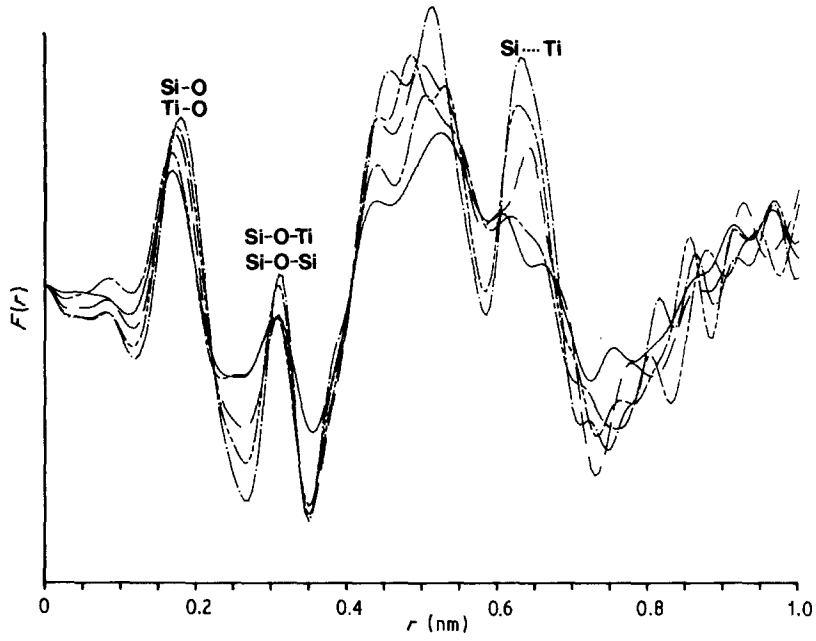


*Figure 3* Experimental RDF curves. 0% Ti (——); 10% Ti (– – –); 20% Ti (— —); 25% Ti (– – – –); 30% Ti (— · — · —).

by the LAXS technique as a function of titanium content. Fig. 3 shows the radial distribution curves (RDF) obtained with the materials prepared by the second procedure up to 30% molar titanium. Several comments can be made

(i) The first peak shifts from 0.170 nm for the titanium-free polysiloxane to 0.180 nm for the 30% titanium material and the peak intensity increases. This modification corresponds to the formation of titanium–oxygen bonds.

(ii) The intensity of the second peak, at 0.310 nm, only increases when the titanium percentage is higher than 20%. This peak corresponds to the Si–O–Si and Si–O–Ti interactions.

(iii) The intensity of the broad peak between 0.400 and 0.550 nm regularly increases with the titanium content. However, it is quite impossible to derive any information about the metal surrounding as a great amount of different interactions are superimposed in this peak.

(iv) The most relevant point in these RDF curves is the evolution of the peak at 0.640 nm, the intensity of which considerably increases. This implies that this distance corresponds to a particular interaction between titanium and other atoms.

This hypothesis can be checked by the following experiments. It is to be seen that the monoliths turn slightly blue when exposed to solar light. This suggests a reduction of Ti(IV) to Ti(III). So, LAXS measurements were done under UV irradiation on titanium free and 20% titanium samples. The corresponding RDF curves are given in Figs 4a and 4b.

The titanium-free material remains colourless during irradiation and there is no change in the local order. On the contrary, the titanium-doped material is light yellow and turns deep blue very quickly. The complete disappearance of this colour is very slow (at least 24 h).The RDF curves show great changes in the 0.4 to 0.7 nm domain. The most remarkable point is, of course, the increase of the peak at 0.640 nm. Its evolution confirms unambiguously that this peak is due to interactions based on titanium atoms.

The behaviour of the materials under UV light has also been studied by EPR spectroscopy. Fig. 5a shows the study of the titanium-free sample. The signal is very weak, whatever the irradiation time, the intensity is constant and the relaxation time very short. The 20% titanium material gives the spectrum shown on Fig. 5b. The signal is much more intense and increases regularly even after 3 h irradiation. The relaxation time is rather long: 55 h to get back the initial spectrum. A thorough study of irradiated titanium containing silicate glasses, by Iwamoto *et al.* [13], suggests that $Ti^{3+}$ ions are in tetragonally distorted octahedral environments.

Thus, the key point to determine the titanium surrounding in the materials is the peak at 0.640 nm in the

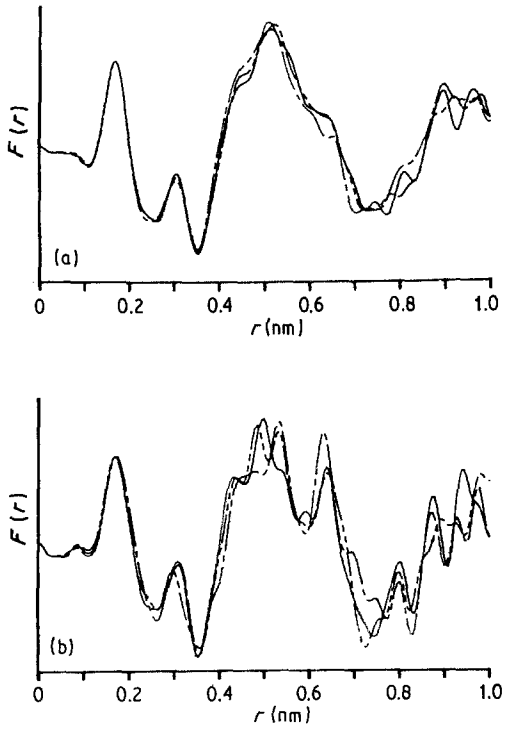


*Figure 4* Evolution of experimental RDF curves with UV irradiation. (a) titanium-free compound; (b) 20% molar Ti compound. Before irradiation (——); after 6 h of irradiation (– – –); after one week of relaxation (– – – –).

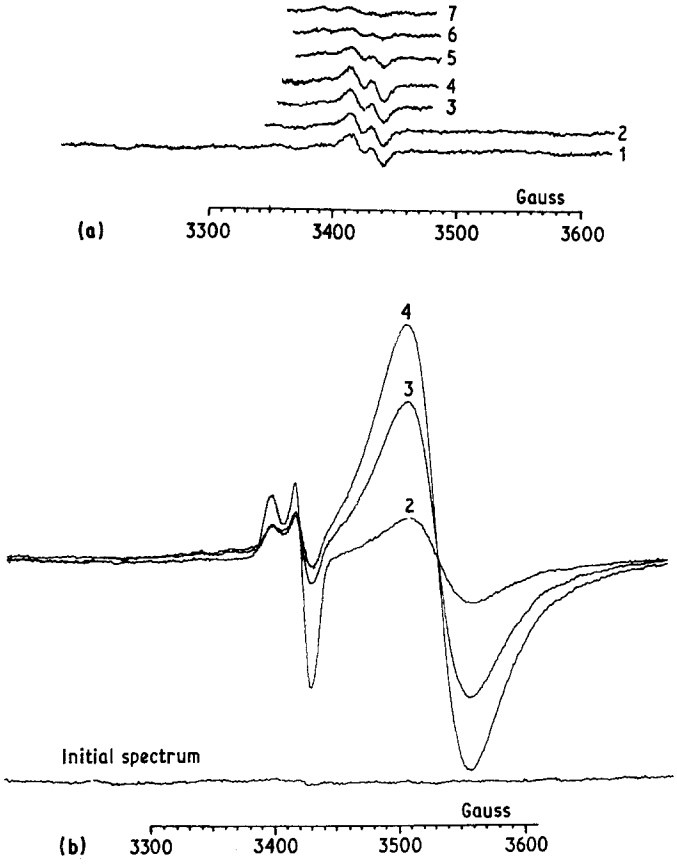


*Figure 5* EPR study under UV irradiation of (a) titanium-free compound. (Relaxation time: 7, 3 min; 6, 2 min; 5, 1 min; irradiation time: 4, 15 min; 3, 7 min; 2, 5 min; 1, 30 sec) and (b) 20% molar titanium compound. (Irradiation time: 4, 10 min; 3, 6 min; 2, 1 min).

RDF curves. The very high intensity of this peak, higher than the coordination peak, suggests the existence of Ti . . . Si interactions. The examination of bond distances and angles in the side chain of the siloxane shows that the coordination of titanium atoms to the diol function leads to the correct Ti . . . Si distance (Fig. 6). This hypothesis is strengthened by the evolution of the peak intensity at 0.310 nm. Indeed, if such Ti . . . Si distances come from a polymeric chain like . . . Si–O–Si–O–Ti . . ., the peak intensity should increase with the titanium content due to the formation of Ti–O–Si bonds. It can, however, be noticed that this intensity increases only when the titanium percentage is higher than 20%. Moreover, the FT–NIR measurements indicate that around 40% of the diol functions are free in the materials. So, a maximum of 30% metallic atoms could be coordinated to two diol functions (or 20% coordinated to three functions).

This discussion leads to the following conclusion: titanium atoms are in an octahedral environment and are preferably coordinated to the diol functions. If the titanium percentage is higher than 20%, the metallic atoms are distributed on several sites with formation of Ti–O–Si bonds.

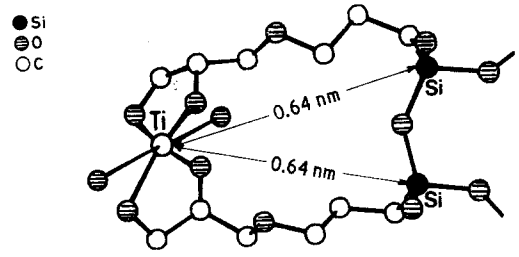


*Figure 6* Coordination of the titanium atoms to the diol function. (● Silicon, ⊜ oxygen, ○ carbon).

## 3.2. Modelling of the siloxane polymer

The scientific literature on polysiloxanes gives very few starting points to build a model, as the structural studies on single crystals are very scarce. Three structural types can be distinguished and checked:

(i) oligomers based on cyclo tri- or tetrasiloxanes [14–17]

(ii) more extended oligomers based on "bowl" models with the side chains expanding outside the bowl. The prototype of these models is the complex anion $\{[(PhSi)_7O_{13}Co]_3\ SiPh\}^{6-}$ [18].

(iii) polymers based on the models proposed for liquid crystalline polysiloxanes [19, 20]. These macromolecules are built up on polymeric chains $(-Si-O-Si-)_n$ with a quasi-parallel arrangement of the aliphatic side chains, giving a comb-like model (Fig. 7).

The first two structural types have been abandoned because of the bad agreement between experimental and calculated RDFs. Particularly, the broad peak between 0.45 and 0.70 nm is not explained.

The third type gives much better results. The model 1 is built up from a $(-Si-O-)_8$ chain with the eight side chains extending perpendicularly to the main chain (Fig. 8). The Si . . . Si distances are equal to 0.310 nm for the consecutive silicon atoms and to 0.50 to 0.55 nm for atoms like $Si_1$ . . . $Si_3$ or $Si_2$ . . . $Si_5$. The calculated RDF curve, compared to the experimental one, reproduces the structural features (0.44–0.51–0.59 nm) in the main peak. Obviously, however, the intensity is too weak.

The fit can be considerably improved if this first model is expanded through the lengthening of the $(-Si-O)_n$ chain and the stacking of two units like model 1. The "sandwich" model 2 (Fig. 9) is built in

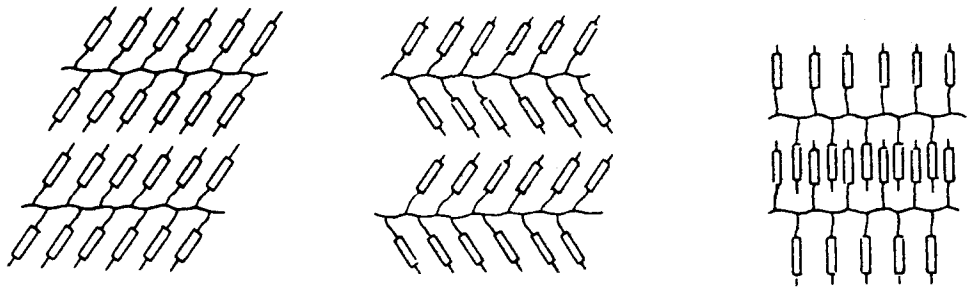

*Figure 7* Schematic drawing of the comb-like models proposed for liquid crystalline polysiloxanes (from [19]).

this way with twelve silicon atoms in the main chain. The corresponding calculated RDF curve shows an acceptable agreement with the experimental one but the relative intensities in the main peak are not properly reproduced.

The only way to get a better fit is to build a model based on a stack of models 2. The so-obtained model 3 gives a rather satisfactory fit, particularly for the broad peak.

Of course, this fit is not perfect and critical comments can be afforded against the proposed model:

(i) The model is paracrystalline. The main chain $(-Si-O-)_n$ is too regular with the silicon and oxygen atoms in the same plane.

(ii) The relative positions of the side chains have not been optimized.

(iii) The stacking periodicity is also too regular. It is possible to change slightly the intensities and positions of the peaks at 0.44, 0.51 and 0.59 nm by adjustment of the relative positions of the layers in the stack. It means that a more random stack would broaden these peaks and lead to a continuous distribution as in the experimental RDF curve.

(iv) Our model is based on a layered structure; there is no chemical bond between the layers, only Van der Waals contacts. This is again an oversimplified view. The layers are probably connected through Si–O–Si bonds or, presumably, through titanium atoms.

However, despite these reservations, the agreement between experimental and calculated data, agreement resulting from a systematic examination and elimination of the different models proposed in the literature, allows to assign a high reliability index to our model.

## 4. Conclusion

The LAXS investigation is sensitive enough to follow structural distorsions induced by UV irradiation of the sample, distorsions corresponding to a $Ti^{4+}$–$Ti^{3+}$ transition.

The local order proposed for these materials is characterized by a layered structure. The skeleton consists in $(-Si(R)-O-)_n$ chains where R is the aliphatic side chain. These side chains are ordered in a quasi-parallel arrangement as in liquid crystalline polysiloxanes.

If the titanium percentage is less than 20%, the metal atoms are preferably coordinated to the diol functions, in an octahedral surrounding. If the titanium percentage is higher, the metal atoms are distributed on several sites with formation of Ti–O–Si bonds.

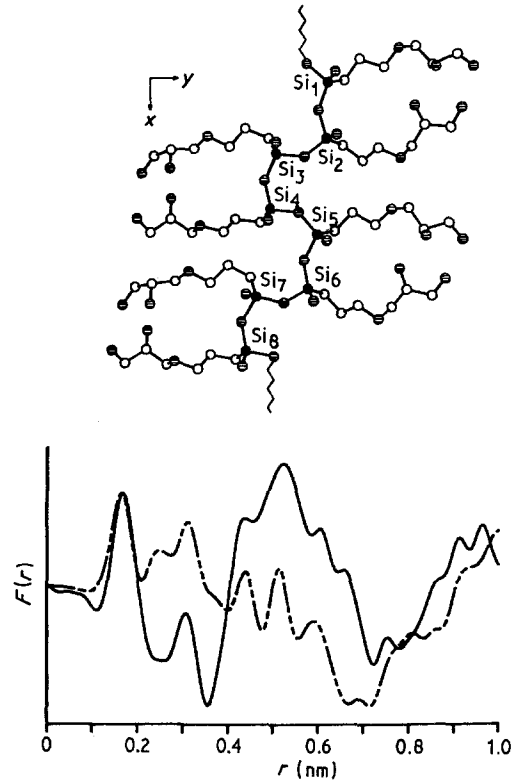


*Figure 8* Model 1 and comparison of the experimental RDF curve (——) for the 20% Ti compound and the calculated one (- - - -). (● silicon, ⊜ oxygen, ○ carbon).

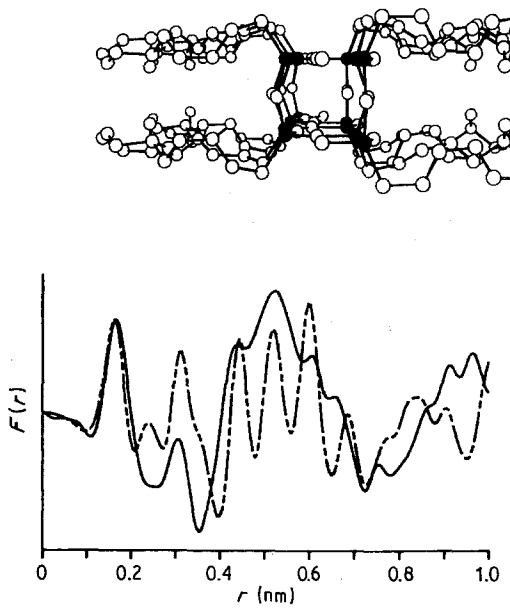


*Figure 9* Model 2 and comparison of the experimental RDF curve (——) and the calculated one (- - - -).

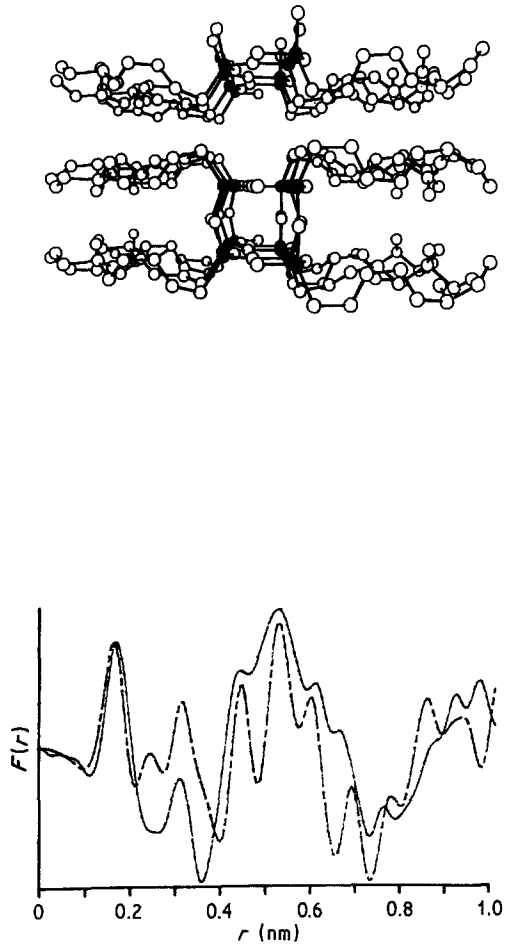


*Figure 10* Model 3 and comparison of the experimental RDF curve (——) and the calculated one (- - -).

## References


1. H. SCHMIDT, *Mater. Res. Soc. Symp. Proc.* **32** (1984) 327.
2. G. PHILIPP and H. SCHMIDT, *J. Non-Cryst. Solids* **82** (1986) 31.
3. H. H. HUANG, B. ORLER and G. L. WILKES, *Polym. Bull.* **14** (1985) 557.
4. J. E. MARK and C. C. SUN, *ibid.* **18** (1987) 259.
5. G. PHILIPP and H. SCHMIDT, *J. Non-Cryst. Solids* **63** (1984) 283.
6. H. SCHMIDT, *ibid.* **73** (1985) 681.
7. P. LECANTE, A. MOSSET and J. GALY, *J. Appl. Crystallogr.* **18** (1985) 214.
8. A. MOSSET, P. LECANTE, J. JAUD and J. GALY, *Spectra 2000* **15** (1987) 33.
9. J. KROGH-MOE, *Acta Crystallogr.* **9** (1956) 951.
10. D. T. CROMER and J. T. WABER, *ibid.* **18** (1965) 104.
11. D. T. CROMER, *J. Chem. Phys.* **50** (1969) 4857.
12. P. DEBYE, *Ann. Phys.* **46** (1915) 809.
13. N. IWAMOTO, H. HIDAKA and Y. MAKINO, *J. Non-Cryst. Solids* **58** (1983) 131.
14. P. E. TOMLINS, J. E. LYDON, D. AKRIGG and B. SHELDRICK, *Acta Crystallogr.* **C41** (1985) 292.
15. W. CLEGG, *ibid.* **B38** (1982) 1648.
16. M. SODERHOLM and D. CALSTROM, *Acta Chem. Scand.* **B31** (1977) 193.
17. M. A. HOSSAIN, M. B. HURTHOUSE and K. M. A. MALIK, *Acta Crystallogr.* **B25** (1979) 522.
18. Yu. E. OUCHINNIKOV, A. A. ZHDANOV, M. M. LEVITSKII, V. E. SHKLOVER and YU. T. STRUCHKOV, *Izv. Akad. Nauk SSSR, Ser. Khim.* **5** (1986) 1206.
19. H. H, SUTHERLAND and A. RAWAS, *Mol. Cryst. Liq. Cryst.* **138** (1986) 179.
20. H. J. COLES and R. SIMON, *ibid.* **1** (1985) 75.



*Received 21 February*
*and accepted 30 August 1989*